PAPER

Ultra high adsorption capacity of fried egg jellyfish-like γ-AlOOH(Boehmite)@SiO₂/Fe₃O₄ porous magnetic microspheres for aqueous Pb(II) removal†

Yong-Xing Zhang,[ab] Xin-Yao Yu,[a] Zhen Jin,[a] Yong Jia,[a] Wei-Hong Xu,[a] Tao Luo,[a] Bang-Jing Zhu,[a] Jin-Huai Liu[*a] and Xing-Jiu Huang[*ac]

Fried egg jellyfish-like γ-AlOOH(Boehmite)@SiO₂/Fe₃O₄ porous magnetic microspheres were synthesized by a simple template-induced method. The products were characterized by X-ray diffraction (XRD) analysis , scanning electron microscopy (SEM), transmission electron microscopy (TEM), X-ray energy dispersive spectrometry (EDS), Fourier transform infrared spectroscopy (FTIR), nitrogen adsorption–desorption techniques and vibrating sample magnetometry (VSM). Influencing factors, such as the concentration of reactants, the reaction temperature and the reaction time, were systematically investigated. The adsorption properties of the fabricated sample were investigated for aqueous Pb(II) removal. The maximum adsorption capacity (q_m) increased rapidly with an increasing void space in the shell of the microspheres, indicating that the void space is beneficial for increasing the adsorption properties of the material. The maximum adsorption capacity, $q_m = 214.59$ mg g^{-1}, is approximately 11.7-fold and 34.6-fold higher than SiO₂/Fe₃O₄ and Fe₃O₄ magnetic microspheres, respectively. The adsorption isotherm fitted the Langmuir model well and the square of the correlation coefficient was $r^2 > 0.996$. In addition, the effects of pH on the adsorption kinetics have also been investigated.

1. Introduction

Because the Earth's water supplies have been contaminated by various organic and inorganic pollutants, thereby posing a major environmental health risk to humankind, water purification technology has attracted much attention recently. Adsorption is one of the most effective and simplest approaches that has been developed for this purpose. The method is reliant on advanced materials, such as porous carbons,[1–7] mesoporous silicas,[8,9] functionalized mesoporous silicas,[10,11] and other mesoporous and hierarchical materials.[12–16] Without question, the development of the adsorption method relies heavily on research progress in the field of adsorbent materials. However, it is very difficult to recycle these materials due to their superior dispersive properties. Furthermore, conventional separation methods, including centrifugation or filtration, may lead to loss of the adsorbent, which may bring about secondary pollution to the

environment. The synthesis of new adsorbents is considered to be of critical importance for the development of handy purifiers for both drinking water and waste water.

Among them, iron oxide-based magnetic adsorbents have been extensively studied due to their special magnetic properties.[17–23] These magnetic adsorbents can be easily separated from aqueous systems by an external magnetic field. Thus, lower operational costs for absorbent separations and recycling of the adsorbent materials could be easily achieved. Magnetic iron oxides can be combined with other materials to obtain multifunctional magnetic adsorbents. However, the combination of different building blocks into an ordered micro/nanostructure is considerably more difficult, especially for components with different porous crystalline structures. Moreover, most magnetic adsorbents have a low maximal adsorption capacity for aqueous heavy metal ion removal because of the introduction of the magnetic core.[19,24] Development of a reliable synthetic method for the fabrication of multifunctional micro/nanocomposites with designed components and controlled morphologies is still a big challenge. Recently, surface coating (or surface modification) has been recognized as one of the most intriguing methods to build complex micro/nanostructures.[20,23] Coating or modification can alter the surface charge and reactivity of the substrate. SiO₂ is a special and unique material used in coating treatments and, *via* its use, core/shell type nanostructures can be achieved. The activated OH groups of SiO₂ can easily be introduced into other

aResearch Center for Biomimetic Functional Materials and Sensing Devices, Institute of Intelligent Machines, Chinese Academy of Sciences, Hefei, 230031, P.R. China. E-mail: xingjiuhuang@iim.ac.cn; jhliu@iim. ac.cn; Fax: +86-551-5592420; Tel: +86-551-5591142

bDepartment of Chemistry, University of Science and Technology of China, Hefei, 230026, P.R. China

cSchool of Mechanical and Electronic Engineering, Wuhan University of Technology, Wuhan, 430070, P.R. China

† Electronic supplementary information (ESI) available. See DOI: 10.1039/c1jm12196k

inorganic materials by controlling the reaction conditions.[20,25,26] As a result, the combination of different building blocks into ordered micro/nanostructures can be achieved.

γ-AlOOH(Boehmite) exhibits a lamellar structure (with orthorhombic symmetry), in which the Al^{3+} ions exist in distorted, edge-sharing octahedral arrays of oxide ions that form a double layer with the layers connected by zigzag chains of H-bonds. Because of the large number of OH groups on the surface, γ-AlOOH is inclined to interact with foreign molecules or heavy metal ions, which allows it to be one of the important adsorbent materials. To date, various morphologies of γ-AlOOH, such as nanoparticles,[27,28] nanofibers,[29,30] nanotubes,[31] thin plates,[32,33] hierarchical flower-like and other structures[34–40] have been successfully prepared. Nevertheless, there are few reports on the preparation of porous magnetic γ-AlOOH micro/nanostructure composites, which are expected to exhibit excellent properties for water treatment. Here, we report that fried egg jellyfish-like γ-AlOOH(Boehmite)@SiO_2/Fe_3O_4 structures with porous shells were synthesized by a simple and robust method. In the experiments, the SiO_2, which was first modified on the surface of the Fe_3O_4 magnetic microspheres, induced the preferential generation and deposition of γ-AlOOH with a porous shell. The void space in the shell of the resulting products can be controlled by tuning the concentration of the reagents. The void space also has an effect on the adsorption capacity of the sample, which was investigated for the removal of Pb(II) from aqueous solutions. At the same time, the influence of pH on the adsorption capacity, isotherm modeling, adsorption kinetics and adsorption efficiency was also studied for the removal of Pb(II) from aqueous solutions.

2. Experimental section

All reagents were of an analytical grade and are commercially available from Sinopharm Chemical Reagent Co., Ltd (China) and were used without further purification.

2.1. Preparation of Fe_3O_4 microspheres

The synthesis was carried out according to a previous report with a small modification.[41] In a typical procedure, 1.35 g of $FeCl_3 \cdot 6H_2O$ was dissolved in 40 mL of ethylene glycol to form a clear solution, then 1.0 g of polyethylene glycol 10 000 and 3.6 g of $NaAc \cdot 3H_2O$ were added. The mixture was stirred until the reactants were fully dissolved. After that, the mixture was transferred to a Teflon-lined autoclave with a capacity of 50 mL and heated at 200 °C for 10 h. The products were separated with a magnet and rinsed with deionized water and ethanol several times each before being dried under vacuum at 50 °C for 6 h prior to further use.

2.2. Preparation of SiO_2/Fe_3O_4 microspheres

The synthesis was carried out according to the Stöber method with a small modification.[42] Typically, 0.4 g of prepared Fe_3O_4 microspheres were dispersed in a mixture of 40 mL ethanol and 8 mL deionized water by ultrasonication for about 10 min. Then, under continuous mechanical stirring, 2 mL of an ammonia solution (25%) and 1.6 mL of tetraethyl orthosilicate (TEOS) were consecutively added to the mixture. The reaction was

allowed to proceed at room temperature for 3.5 h under continuous mechanical stirring with ultrasonication. The resulting products were collected and washed, and then dried under vacuum at 60 °C for 3 h prior to further use.

2.3. Preparation of fried egg jellyfish-like γ-AlOOH (Boehmite)@SiO_2/Fe_3O_4 microspheres

The synthesis process of fried egg jellyfish-like γ-AlOOH (Boehmite)@SiO_2/Fe_3O_4 microspheres is described briefly as follows. The SiO_2/Fe_3O_4 microspheres (0.14 g) were dispersed to form a homogeneous suspension in 20 mL of deionized water by ultrasonication. 0.68 g of sodium aluminate ($NaAlO_2$) and 1.92 g of urea (NH_2CONH_2) were dissolved in 30 mL of deionized water by stirring. The above solutions were then mixed to form a homogeneous suspension and transferred to a Teflon autoclave (70 mL) and heated to a temperature of 160 °C for 12 h. After cooling to room temperature, the precipitate was collected and washed with deionized water, and then the product was dried in a vacuum oven at 50 °C for 6 h.

2.4. Pb(II) removal experiments

$Pb(NO_3)_2$ was used as the source of Pb(II). The different concentrations of Pb(II) ions were prepared and the different pH values of the solutions were adjusted by addition of HNO_3. The adsorbent dose was 1 g L^{-1} in the solution. The mixtures were shaken at a speed of 100 rpm for some hours to establish an adsorption equilibrium at 298 K. The adsorbent was then separated from the mixture by a magnet. Adsorption isotherms were measured in batch experiments at pH = 5.0 for 24 h. The adsorption kinetic experiments were carried out inside 50 mL stoppered conical flasks containing 1 g L^{-1} adsorbent and various concentrations of Pb(II) ions. The samples were collected at desired time intervals and separated by a magnet immediately. The amount of metal adsorbed (q_e) was determined by the following equation:

$$q_e = \frac{(C_0 - C_e)V}{m} \tag{1}$$

where C_0 and C_e represent the initial and equilibrium metal ion concentrations (mg L^{-1}), respectively; V is the volume of the solutions (mL) and m is the amount (mg) of adsorbent.

2.5. Characterization

Field emission scanning electron microscope (FESEM) images were taken on a FESEM (Quanta 200 FEG) operated at an accelerating voltage of 10.0 kV. Transmission electron microscope (TEM) images were obtained on a JEOL JEM-2010 high resolution transmission electron microscope, equipped with X-ray energy dispersive spectroscopy (EDS) capabilities, working at an acceleration voltage of 200 kV. Fourier transform infrared spectroscopy (FTIR) was performed on a Nicolet iS10 Fourier transform IR (FTIR) spectrometer at room temperature. The samples and KBr crystals were ground together and the mixture pressed into a flake for IR spectroscopy. X-Ray scattering patterns were conducted by analyzing the powder samples on a Philips X'Pert Pro X-ray diffractometer (XRD) with Cu Kα radiation (1.5418 Å). The specific surface

areas of the as-prepared products were measured with Micromeritics ASAP 2020 M+C Brunauer–Emmet–Teller (BET) equipment by using nitrogen adsorption and desorption. The magnetic properties of the samples were investigated by using a vibrating sample magnetometer (VSM) with an applied field between −5000 and 5000 Oe at room temperature (BHV-55, Riken, Japan). To determine Pb(II) ion removal by the adsorbent, the Pb(II) concentration in the remaining solution was measured by an inductively coupled plasma atomic emission spectrophotometer (ICP-AES, Jarrell-Ash, model ICAP 9000).

3.   Results and discussion

3.1.   Characterization of synthesized magnetic adsorbents

Powder XRD was used to monitor the phase structure of the as-prepared products (Fig.1). In an XRD pattern of the obtained Fe_3O_4 sample (curve a), all the diffraction peaks could be easily indexed to the standard Fe_3O_4 reflections (JCPDS card No. 75–1609). Curve b is a typical XRD pattern of the SiO_2/Fe_3O_4 microspheres, which show almost all the same features as those shown in curve a. No diffraction peaks corresponding to SiO_2 were observed, which was due to the fact that the prepared SiO_2 is amorphous. In comparison to the XRD patterns of the SiO_2/Fe_3O_4 shell/core microspheres and Fe_3O_4 microspheres, four additional peaks at 14.2°, 27.8°, 38.3°, 49.1° and 64.1° were observed in curve c, which represent the Bragg reflections from the (020), (120), (031), (200) and (231) planes of orthorhombic γ-AlOOH(Boehmite) (JCPDS card 21–1307), showing clearly the immobilization of γ-AlOOH(Boehmite) onto the surface of the SiO_2/Fe_3O_4 shell/core microspheres.

Fig. 2a shows the SEM image of the Fe_3O_4 microspheres, from which it can be clearly seen that the sample is composed of many nearly monodispersed spherical particles with a diameter of about 400 nm. An SEM image of the SiO_2/Fe_3O_4 microspheres is shown in Fig. 2b, which indicates that the microspheres have a smooth SiO_2 shell. Fig. 2c displays the SEM image of the fried egg jellyfish-like γ-AlOOH(Boehmite)@SiO_2/Fe_3O_4 microspheres. The shell and the magnetic core of the sample can be

Fig. 2   SEM images of (a) Fe_3O_4 microspheres, (b) SiO_2/Fe_3O_4 microspheres, and (c) fried egg jellyfish-like γ-AlOOH(Boehmite)@SiO_2/Fe_3O_4 microspheres; (d) high-magnification SEM image collected from panel c. The inset is a digital photograph of a real fried egg jellyfish obtained from the internet.[49]

clearly seen. The morphology of the microspheres is very similar to that of a fried egg jellyfish. It is worth mentioning that the SiO_2 shell is the key factor for preparing fried egg jellyfish-like γ-AlOOH(Boehmite)@SiO_2/Fe_3O_4 microspheres. It induces the preferential generation and deposition of γ-AlOOH on the SiO_2/Fe_3O_4 microsphere templates.[25] A clear image of the fried egg jellyfish-like γ-AlOOH(Boehmite)@SiO_2/Fe_3O_4 microspheres can be seen in Fig. 2d.

Further information about the synthesized structures is found by looking at the TEM images. By comparison with the shell/core structure of the SiO_2/Fe_3O_4 microspheres (Fig. 3a), a clear boundary between the SiO_2 shell, the Fe_3O_4 core and a void space are observed in the fried egg jellyfish-like structures (Fig. 3b), as is evident in the inset image of Fig. 3b. Furthermore, the high-magnification TEM image (Fig. 3c) shows that there are many mesopores (indicated by the circles) in the shell of the as-prepared sample. The void space and mesoporous structures are helpful in increasing the BET surface area and the adsorption capacity of the sample, as will be discussed in the following section. The inset image of Fig. 3c shows that the shell structure is assembled by many nanoparticles. Fig. 3d is the EDS of the fried egg jellyfish-like γ-AlOOH(Boehmite)@SiO_2/Fe_3O_4 microspheres, in which Fe, Al, Si, and O are all present. The Cu signal originates from the copper TEM grid.

Fig. 4 shows the N_2 physisorption experiments and the corresponding N_2 adsorption–desorption isotherms and pore size distributions. It can be seen that the fried egg jellyfish-like γ-AlOOH(Boehmite)@SiO_2/Fe_3O_4 microsphere sample has a type IV isotherm with a type H3 hysteresis loop, which is characteristic of mesoporous materials (according to the IUPAC classification).[43] The typical IV-shaped isotherms indicate that slit-shaped pores are present in the fried egg jellyfish-like γ-AlOOH(Boehmite)@SiO_2/Fe_3O_4 microsphere sample, which may derive from the interspaces of nanoparticles and their surface gaps. Apparently, the porosity of Fe_3O_4 and SiO_2/Fe_3O_4 microspheres is less than the porosity of this sample. The hysteresis loops of the fried egg jellyfish-like γ-AlOOH

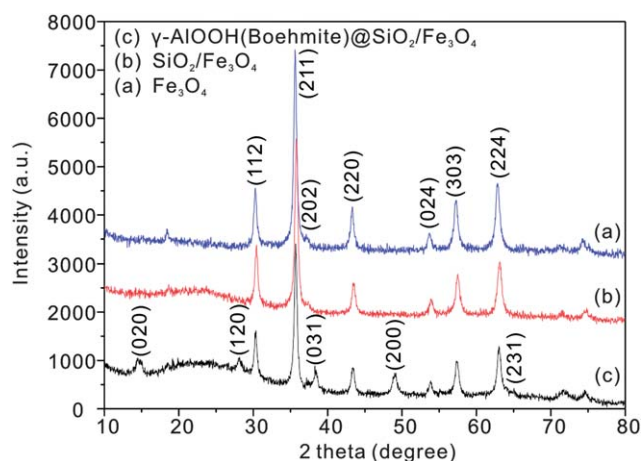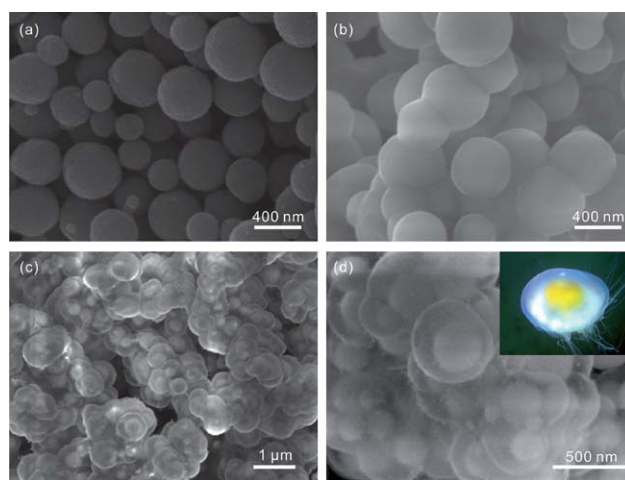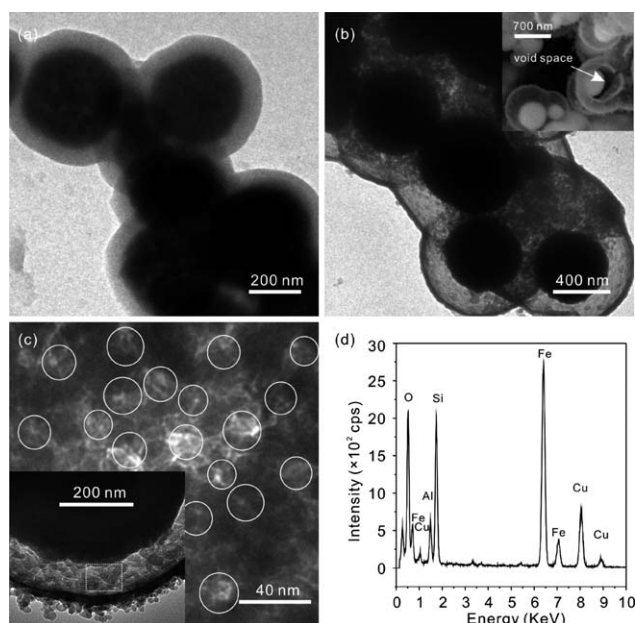**Fig. 1**   Powder X-ray diffraction (XRD) patterns of (a) Fe_3O_4 microspheres (b) SiO_2/Fe_3O_4 microspheres, and (c) fried egg jellyfish-like γ-AlOOH(Boehmite)@SiO_2/Fe_3O_4 microspheres.

Fig. 3 TEM image of (a) SiO_2/Fe_3O_4 microspheres and (b) fried egg jellyfish-like γ-AlOOH(Boehmite)@SiO_2/Fe_3O_4 microspheres. The inset image in panel b is a SEM image showing the void space in the sample (indicated by the arrow). (c) High-magnification TEM image showing many mesopores (indicated by the circles) in the shell structure (indicated by a white square) of fried egg jellyfish-like γ-AlOOH(Boehmite)@SiO_2/Fe_3O_4 microspheres. The inset image is a TEM image of the shell structure of the sample. (d) EDS analysis for fried egg jellyfish-like γ-AlOOH(Boehmite)@SiO_2/Fe_3O_4 microspheres.
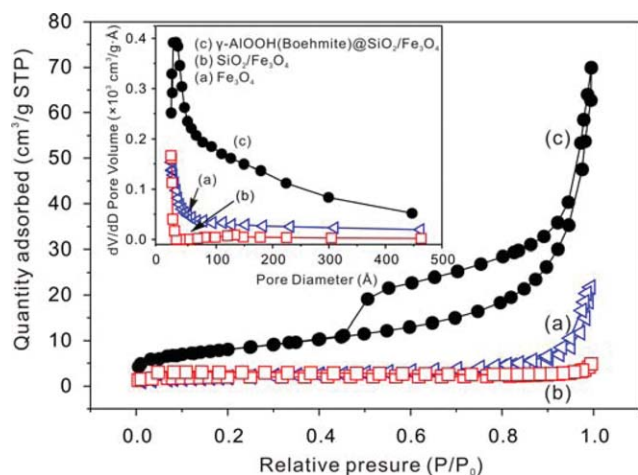

Fig. 4 Nitrogen adsorption–desorption isotherms and the corresponding pore-size distribution curves (inset) for the samples: a) Fe_3O_4 microspheres, b) SiO_2/Fe_3O_4 microspheres, c) fried egg jellyfish-like γ-AlOOH(Boehmite)@SiO_2/Fe_3O_4 microspheres.

(Boehmite)@SiO_2/Fe_3O_4 microsphere samples in a lower relative pressure range ($0.45 < P/P_0 < 0.9$) are related to fine intra-aggregated pores in the shells of primary agglomerated nanoparticles. In the higher relative pressure range ($0.9 < P/P_0 < 1$), the hysteresis loops are associated to larger inter-aggregated pores between secondary aggregated particles. This bimodal mesopore-size distribution has been further confirmed by the

corresponding pore-size distributions (inset in Fig. 4). The sample contains small intra-aggregated mesopores with a peak pore diameter of *ca.* 2.8 nm and larger inter-aggregated mesopores (the large pore diameter size distribution is relatively wide). The smaller mesopores reflect porosity within the γ-AlOOH (Boehmite) shells, while larger mesopores can be related to the pores formed between aggregated fried egg jellyfish-like γ-AlOOH(Boehmite)@SiO_2/Fe_3O_4 microspheres and the void space in the shell of the sample, as observed by SEM and TEM. The quantitative textural information of the as-synthesized samples is summarized in Table S1†.

Fig. 5 shows a comparison of the magnetic hysteresis loops. As can be seen, the magnetic saturation (M_s) values of the Fe_3O_4 microspheres, SiO_2/Fe_3O_4 microspheres, and fried egg jellyfish-like γ-AlOOH(Boehmite)@SiO_2/Fe_3O_4 microspheres are 65.4, 40.1, and 28.3 emu g^{-1}, respectively. The lower M_s values of SiO_2/Fe_3O_4 and γ-AlOOH(Boehmite)@SiO_2/Fe_3O_4 microspheres are due to the layer of amorphous SiO_2 and γ-AlOOH (Boehmite)@SiO_2 outside the Fe_3O_4 microspheres, respectively. Furthermore, it can be seen from the enlarged view of the central loop of the samples (Fig. S1†) that there is no significant change in the coercivity. Such excellent magnetic properties imply a strong magnetic responsivity of the microspheres, which enables them to be recycled easily from solution by application of an external magnetic force. A complete magnetic separation test for fried egg jellyfish-like γ-AlOOH(Boehmite)@SiO_2/Fe_3O_4 microspheres can be seen in the inset of Fig. 5. Additional confirmation of the structure and composition of the γ-AlOOH(Boehmite)@SiO_2/Fe_3O_4 microspheres was carried out using FTIR spectra, see Supplementary Information for details (Fig. S2†).

3.2. Effect of the concentration of reactants on the synthesized magnetic adsorbents

To better understand the formation of fried egg jellyfish-like γ-AlOOH(Boehmite)@SiO_2/Fe_3O_4 microspheres, the effect of

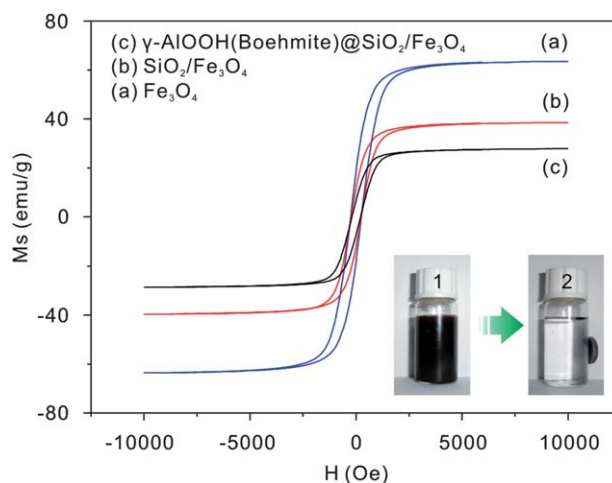**Fig. 5** Magnetic hysteresis loops for a) Fe_3O_4 microspheres, b) SiO_2/Fe_3O_4 microspheres and c) fried egg jellyfish-like γ-AlOOH(Boehmite)@SiO_2/Fe_3O_4 microspheres. The inset images are digital photographs of 1) an aqueous solution of Pb(II) with dispersed fried egg jellyfish-like γ-AlOOH(Boehmite)@SiO_2/Fe_3O_4 microspheres, 2) the solution after magnetic separation using an external magnetic field.

the concentration of reactants was investigated. At a lower reactant concentration, many nanopores were observed on the surface of the microspheres (Fig. 6a and the inset image). Following an increase in the concentration, the shell became thick and more nanopores were seen (Fig. 6b and the inset image). As the concentration was increased further, part of the SiO$_2$ shell dissolved and a void space was observed. As can be seen in Fig. 6c, the SiO$_2$ shell almost disappeared and γ-AlOOH (Boehmite) was directly immobilized on the Fe$_3$O$_4$ core. When the concentration of the reagents reached a maximum in our experiments, the void space between the shell and the core became even larger (Fig. 6d). It is concluded that higher concentrations of reactants are beneficial in the synthesis of fried egg jellyfish-like γ-AlOOH(Boehmite)@SiO$_2$/Fe$_3$O$_4$ microspheres. This result was confirmed by SEM as shown in Fig. S3†.

The influence of two other important factors (reaction temperature and time) on the microsphere morphology was also examined. Fig. S4† shows the SEM images of the products from reactions performed at different temperatures with fixed reactant concentrations (*i.e.*, SiO$_2$/Fe$_3$O$_4$, 2.8 g L^{-1}; NaAlO$_2$, 13.6 g L^{-1}; NH$_2$CONH$_2$, 38.4 g L^{-1}) for 12 h. As can be seen, there is no obvious change in the morphology of the magnetic microspheres. A series of time-dependent experiments with fixed reactant concentrations (SiO$_2$/Fe$_3$O$_4$, 2.8 g L^{-1}; NaAlO$_2$, 13.6 g L^{-1}; NH$_2$CONH$_2$, 38.4 g L^{-1}) at 160 °C were conducted and the results are presented in Fig. S5†. Surprisingly, the morphology of the magnetic microspheres does not change with time. These experiments suggest that reaction temperature and time do no have a significant influence on the synthesis of fried egg jellyfish-like γ-AlOOH(Boehmite)@SiO$_2$/Fe$_3$O$_4$ microspheres.
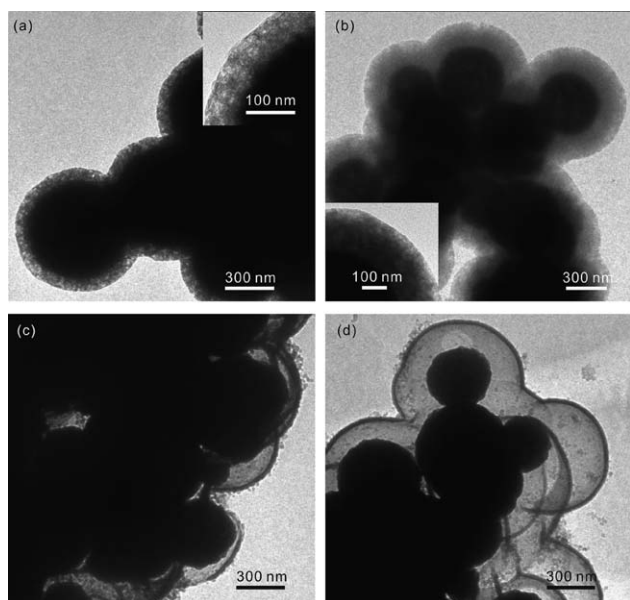

Fig. 6 TEM images of the products obtained with different reactant concentrations under hydrothermal conditions at 160 °C for 12 h. (a) Sample 1. (b) Sample 2. (c) Sample 3. (d) Sample 4. The reactant concentrations corresponding to these samples are shown in Table S2†. The inset images in (a) and (b) show the high magnification TEM images of the porous structures.

3.3. Ultra high adsorption capacity for aqueous Pb(II) removal

The as-prepared microspheres were employed to adsorb Pb(II) from an aqueous solutions at pH = 5 and T = 298 K in our experiment. To ensure that the adsorption equilibrium was reached, the microspheres were incubated in a Pb(II) solution for 24 h. The amount of Pb(II) removed from the solution was considered to have been absorbed by Fe$_3$O$_4$ microspheres, SiO$_2$/Fe$_3$O$_4$ microspheres, and fried egg jellyfish-like γ-AlOOH (Boehmite)@SiO$_2$/Fe$_3$O$_4$ microspheres (Sample 4 was used throughout unless otherwise stated). As shown in the adsorption isotherms (Fig. 7), the performance of fried egg jellyfish-like γ-AlOOH(Boehmite)@SiO$_2$/Fe$_3$O$_4$ microspheres is superior to that of SiO$_2$/Fe$_3$O$_4$ microspheres and Fe$_3$O$_4$ microspheres (the performances of which are shown in the inset of Fig. 7). For example, at a Pb(II) concentration of 86.32 mg g^{-1}, the adsorption capacity of fried egg jellyfish-like γ-AlOOH(Boehmite)@ SiO$_2$/Fe$_3$O$_4$ microspheres could reach 86.31 mg g^{-1}, while only 18.20 mg g^{-1} and 5.93 mg g^{-1} were achieved for Fe$_3$O$_4$ microspheres and SiO$_2$/Fe$_3$O$_4$ microspheres, respectively.

The Langmuir model (eq. (2)) was chosen to fit the adsorption isotherms:

$$q_e = \frac{q_m K_L C_e}{1 + K_L C_e} \qquad (2)$$

where q_e (mg g^{-1}), q_m (mg g^{-1}), C_e (mg L^{-1}) and K_L (L mg^{-1}) are the amount of Pb(II) adsorbed, the maximum adsorption capacity, the equilibrium concentration and the adsorption constant, respectively. It was found that the adsorption fitted well to the Langmuir model with the square of the correlation coefficient r^2 > 0.996 (Fig. S6†). The detailed Langmuir isotherm parameters are listed in Table S3†. The maximum adsorption capacity, q_m = 214.59 mg g^{-1}, for fried egg jellyfish-like γ-AlOOH(Boehmite)@SiO$_2$/Fe$_3$O$_4$ microspheres is approximately 11.7-fold and 34.6-fold higher than those for SiO$_2$/Fe$_3$O$_4$ microspheres and Fe$_3$O$_4$ microspheres, respectively. The high q_m
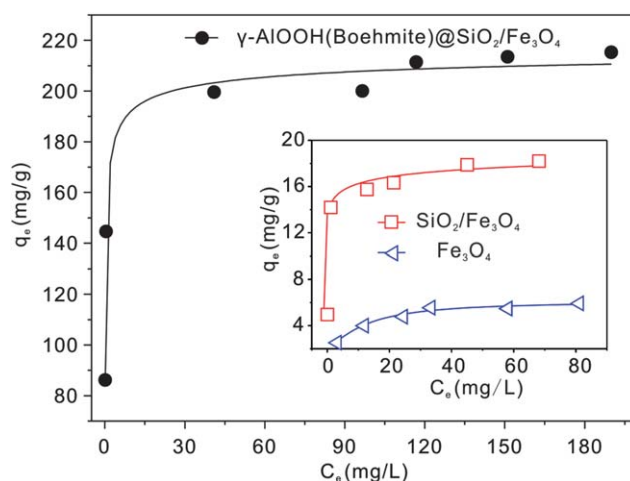

Fig. 7 Adsorption isotherm of fried egg jellyfish-like γ-AlOOH (Boehmite)@SiO$_2$/Fe$_3$O$_4$ microspheres for aqueous Pb(II). The inset image shows the adsorption isotherms of Fe$_3$O$_4$ microspheres (blue triangles) and SiO$_2$/Fe$_3$O$_4$ microspheres (red squares) for aqueous Pb(II). Adsorbent dose = 1 g L^{-1}, shaking rate = 100 rpm, contact time = 24 h, T = 298 K, and pH = 5.

for the sample can be attributed to the porous structure of γ-AlOOH(Boehmite) on the surface of the Fe_3O_4 microspheres. In addition, fried egg jellyfish-like γ-AlOOH(Boehmite)@SiO_2/Fe_3O_4 microspheres also have a good adsorption constant (Table S3†). For comparison, the maximum adsorption capacity of boehmite particles (without SiO_2/Fe_3O_4 microspheres) was found to 65.45 mg g^{-1} (Fig.S7†).

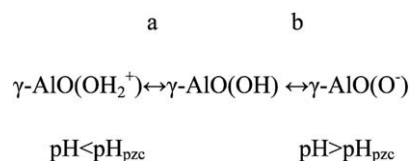We compared the q_m for fried egg jellyfish-like γ-AlOOH(Boehmite)@SiO_2/Fe_3O_4 microspheres with those reported previously using different magnetic absorbents[19,23,44–46] and activated carbon,[46] as shown in Table 1. It can be seen that the sample has the best maximum adsorption capacity of all the magnetic absorbents. The mesoporous structure of the shell of fried egg jellyfish-like γ-AlOOH(Boehmite)@SiO_2/Fe_3O_4 microspheres is responsible for the ultra high adsorption capacity. It should also be noted that the q_m for fried egg jellyfish-like γ-AlOOH(Boehmite)@SiO_2/Fe_3O_4 microspheres is about 10-fold higher than that of activated carbon.[46] The maximal adsorption capacity of the microspheres is also better than that of other non-magnetic absorbents.[24] Thus, it is suggested that the magnetic absorbent has an ultra high adsorption capacity for aqueous Pb(II) removal.

The pH is a significant factor in determining the form of the metallic species in aqueous media. It influences the adsorption process of metal ions as it determines the magnitude and sign of the charge on the ions. The distribution of Pb(II) species as a function of pH is displayed in Fig. S8a†. In the case of a lower pH (<6), positively charged Pb(II) species are dominant. In the case of higher pH values (pH = 7–11), however, there are several Pb(II) species present with different charges. These include Pb(OH)$^+$ and Pb(OH)$_2$, and thus the removal of Pb(II) may possibly be accomplished by the simultaneous precipitation of Pb(OH)$_2$ and the adsorption of Pb(OH)$^+$. Furthermore, pH is also one of the most important parameters for controlling the surface charge of the adsorbents. In this experiment, the influence of pH on the adsorption capacity was studied over a range of pH values from 2 to 6 and not more than 6 to avoid lead precipitation. As shown in Fig. S8b†, it was observed that Pb(II) adsorption increased when the pH increased from 2 to 6 for fried egg jellyfish-like γ-AlOOH(Boehmite)@SiO_2/Fe_3O_4 microspheres. When the pH value is about 4, the adsorption capacity of the adsorbent almost reaches a maximum. This result indicates that the adsorption ability of the sample for Pb(II) is strong in near-neutral conditions and poor in strongly acidic conditions. The Pb(II) adsorption for Fe_3O_4 and SiO_2/Fe_3O_4 microspheres shows the same trend. However, the adsorption abilities of Fe_3O_4 microspheres and SiO_2/Fe_3O_4 microspheres are far lower than that of fried egg

jellyfish-like γ-AlOOH(Boehmite)@SiO_2/Fe_3O_4 microspheres, which confirms that the adsorption effect is due to the γ-AlOOH (Boehmite) layer on the surface of the microspheres.

The adsorption mechanism of lead ions can be explained as follows:

The reactivity of γ-AlOOH(Boehmite) is regulated by its surface properties, such as composition and structural perfection, which depend highly on its environment and the cleaving conditions. The adsorption properties of γ-AlOOH(Boehmite) are based on the presence of the functional groups. In aqueous environments, due to γ-AlOOH(Boehmite) having a large number of surface hydroxyl groups, the adsorption processes can be understood as the reaction of dissolved species with these groups. The groups cause the surface to act as a Lewis base due to the terminal OH sites. In general terms, the chemistry that occurs at the surfaces of these amphoteric oxides is dominated by acid–base interactions. The acid–base behavior of the surface hydroxyl groups can be represented by the following equation:

$$\underset{pH<pH_{pzc}}{\underset{a}{\gamma\text{-AlO(OH}_2{}^+)}} \leftrightarrow \gamma\text{-AlO(OH)} \leftrightarrow \underset{pH>pH_{pzc}}{\underset{b}{\gamma\text{-AlO(O}^-)}}$$

a corresponds to the equilibrium in acidic conditions, b to the equilibrium in basic conditions, and pH_{pzc} is the point of zero charge, where the sum of the positive and negative charges is zero.

Because the pH_{pzc} for γ-AlOOH is in the pH range of 7.4 to 8.8,[47] the material's surface groups are protonated in a weakly acidic medium (at a solution pH < pH_{pzc}). A positive charge develops on the surface of the γ-AlOOH of the material as follows:

$$\gamma\text{-AlOOH} + \text{H–OH} \rightarrow \gamma\text{-AlO(OH}_2{}^+) + \text{OH}^-$$
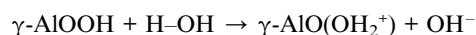
At a solution pH > pH_{pzc}, the hydroxyl surface groups are deprotonated and the surface of the material becomes negatively charged as follows:

$$\gamma\text{-AlOOH} + \text{OH}^- \rightarrow \gamma\text{-AlO(O}^-) + \text{H}_2\text{O}$$
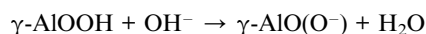
In our experiment, the material was dispersed in a weakly acidic solution (pH = 5). At pH = 5, lead is present as Pb^{2+} in the solution (see Fig. S8†). Lead adsorption must occur not only by electrostatic attraction, but also by a chemical interaction with enough energy to overcome the repulsive forces between the

Table 1 Comparison of the maximum adsorption capacities for fried egg jellyfish-like γ-AlOOH(Boehmite)@SiO_2/Fe_3O_4 microspheres with other magnetic adsorbents and activated carbon as previously reported.

Metal ion	Adsorbent	q_m(mg g^{-1})	Reference
Pb(II)	Iron oxide nanoparticles	36.00	44
	NH$_2$–SiO_2/Fe_3O_4	76.60	45
	Humic acid/Fe_3O_4	92.40	19
	Magnetic carbonaceous nanoparticles	123.10	23
	Activated carbon	22.70	46
	γ-AlOOH(Boehmite)@SiO_2/Fe_3O_4 microspheres	214.59	This study

positively charged composite material surface and the lead ions. Therefore, Pb^{2+} was adsorbed on the composite material by a complexation mechanism at the surface. The formation of complexes at the surface has been previously explained as the reaction mechanism which occurs at solid/solution interfaces.[48] Consequently, the major adsorption schemes may be written as follows:

$$^1/_2\ Pb^{2+} + \gamma\text{-AlO}(OH_2^+) \rightarrow \gamma\text{-AlO}(OPb_{1/2}) + 2H^+$$
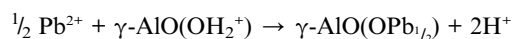
3.4. Effect of contact time and initial Pb(II) concentration

Fig. 8 shows the adsorption capacity (q_t, mg g^{-1}) of Pb(II) by fried egg jellyfish-like γ-AlOOH(Boehmite)@SiO$_2$/Fe$_3$O$_4$ microspheres as a function of time at $T = 298$ K and pH = 5. The initial Pb(II) concentrations were 86.32 and 296.4 mg L^{-1}. As seen in the figure, aqueous Pb(II) was adsorbed onto the sample quickly, and an equilibrium was achieved within 12 min when the initial concentration of Pb(II) (86.32 mg L^{-1}) was lower than that of the maximum adsorption capacity. This may be due to external adsorption dominating with no pore diffusion phenomenon observed, which would slow down the adsorption rate.[44] However, the q_t increases sharply with an increasing contact time, indicating a very rapid adsorption reaction between Pb(II) and the solid surface up to a time of 24 min. This slowed at $t > 24$ min when the initial concentration of Pb(II) was higher than that of the maximum adsorption capacity (296.4 mg L^{-1}). This could be due to the porous structure of the surface of the as-prepared sample and is consistent with the high magnification TEM observations and analysis of the pore size distribution of the samples, which was unfavorable towards the diffusion of Pb(II) ions from the bulk solution to the active sites at the solid surface. The faster initial reaction up to a time of 24 min was due to the rapid diffusion of solute through the boundary surface at the liquid–solid interface by columbic attractions. The slow reaction at $t > 24$ min was presumably due to the columbic/steric hindrance between the solute species sorbed at initial stages by the sorbent surface and the solute remaining for adsorption in solution. Alternatively, it may be due to the reduced concentration of the solute in the liquid phase, which had failed to cross the diffusion barrier at the solid–liquid boundary layer.

4. Conclusions

In summary, fried egg jellyfish-like γ-AlOOH(Boehmite)@SiO$_2$/Fe$_3$O$_4$ microspheres with a unique porous structure were synthesized. The sample possesses a high BET surface area and more pore channels. The product also displays excellent magnetic properties at room temperature. The as-prepared microspheres were employed in the adsorbtion of Pb(II), which shows that they have an ultra high adsorption capacity and efficiency. All of these splendid properties mean that the as-prepared microspheres can be used as novel, highly efficient and fast separation sorbents for the removal of heavy metal ions from waste water.

Acknowledgements

References

1 C. Song, J. P. Du, J. H. Zhao, S. A. Feng, G. X. Du and Z. P. Zhu, *Chem. Mater.*, 2009, **21**, 1524.
2 B. L. Su, A. Vantomme, L. Surahy, R. Pirard and J. P. Pirard, *Chem. Mater.*, 2007, **19**, 3325.
3 X. Q. Wang, J. S. Lee, C. Tsouris, D. W. DePaoli and S. Dai, *J. Mater. Chem.*, 2010, **20**, 4602.
4 Y. Jung, H. I. Lee, J. H. Kim, M. H. Yun, J. Hwang, D. H. Ahn, J. N. Park, J. H. Boo, K. S. Choi and J. M. Kim, *J. Mater. Chem.*, 2010, **20**, 4663.
5 A. Stein, Z. Y. Wang and M. A. Fierke, *Adv. Mater.*, 2009, **21**, 265.
6 Q. C. Zeng, D. C. Wu, C. Zou, F. Xu, R. W. Fu, Z. H. Li, Y. R. Lianga and D. S. Su, *Chem. Commun.*, 2010, **46**, 5927.
7 C. Zou, D. C. Wu, M. Z. Li, Q. C. Zeng, F. Xu, Z. Y. Huang and R. W. Fu, *J. Mater. Chem.*, 2010, **20**, 731.
8 J. Liu, S. B. Hartono, Y. G. Jin, Z. Li, G. Q. Lu and S. Z. Qiao, *J. Mater. Chem.*, 2010, **20**, 4595.
9 M. H. Yu, H. N. Wang, X. F. Zhou, P. Yuan and C. Z. Yu, *J. Am. Chem. Soc.*, 2007, **129**, 14576.
10 K. C. Kao, C. H. Lee, T. S. Lin and C. Y. Mou, *J. Mater. Chem.*, 2010, **20**, 4653.
11 X. Zhuang, Q. F. Zhao and Y. Wan, *J. Mater. Chem.*, 2010, **20**, 4715.
12 J. G. Yu, B. Cheng, Y. Le and W. Q. Cai, *J. Hazard. Mater.*, 2011, **185**, 889.
13 F. N. Gu, F. Wei, J. Y. Yang, N. Lin, W. G. Lin, Y. Wang and J. H. Zhu, *Chem. Mater.*, 2010, **22**, 2442.
14 Y. L. Zhang, S. Wei, Y. Y. He, F. Nawaz, S. Liu, H. Y. Zhang and F. S. Xiao, *J. Mater. Chem.*, 2010, **20**, 4609.
15 B. Zhao and M. M. Collinson, *Chem. Mater.*, 2010, **22**, 4312.
16 A. R. Studart, J. Studer, L. Xu, K. Yoon, H. C. Shum and D. A. Weitz, *Langmuir*, 2011, **27**, 955.
17 J. Liu, S. Z. Qiao, Q. H. Hu and G. Q. (Max) Lu, *Small*, 2011, **7**, 425.
18 J. S. Hu, L. S. Zhong, W. G. Song and L. J. Wan, *Adv. Mater.*, 2008, **20**, 2977.
19 J. F. Liu, Z. S. Zhao and G. B. Jiang, *Environ. Sci. Technol.*, 2008, **42**, 6949.
20 J. Dong, Z. H. Xu and S. M. Kuznicki, *Adv. Funct. Mater.*, 2009, **19**, 1268.
21 P. Wang and I. M. C. Lo, *Water Res.*, 2009, **43**, 3727.
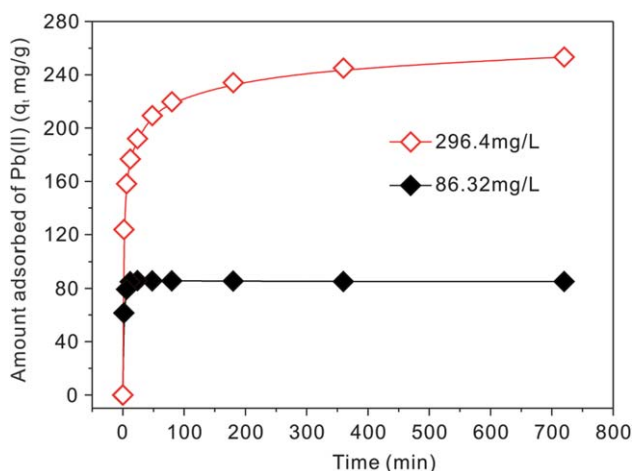22 Y. Deng, D. Qi, C. Deng, X. Zhang and D. Zhao, *J. Am. Chem. Soc.*, 2008, **130**, 28.

Fig. 8 Effect of contact time on the removal of aqueous Pb(II) at different initial concentrations for fried egg jellyfish-like γ-AlOOH(Boehmite)@SiO$_2$/Fe$_3$O$_4$ microspheres. Adsorbent dose = 1 g L^{-1}, shaking rate = 100 rpm, $T = 298$ K, and pH = 5.

23 I. F. Nata, G. W. Salim and C. K. Lee, *J. Hazard. Mater.*, 2010, **183**, 853.
24 J. Zheng, B. H. Wu, Z. Y. Jiang, Q. Kuang, X. L. Fang, Z. X. Xie, R. B. Huang and L. S. Zheng, *Chem-Asian J.*, 2010, **5**, 1439.
25 Y. Q. Wang, G. Z. Wang, H. Q. Wang, W. P. Cai, C. H. Liang and L. Zhang, *Nanotechnology*, 2009, **20**, 155604.
26 P. M. Arnal, C. Weidenthaler and F. Schuth, *Chem. Mater.*, 2006, **18**, 2733.
27 Y. Mathieu, B. Lebeau and V. Valtchev, *Langmuir*, 2007, **23**, 9435.
28 R. W. Hicks and T. J. Pinnavaia, *Chem. Mater.*, 2003, **15**, 78.
29 S. C. Kuiry, E. Megen, S. A. Patil, S. A. Deshpande and S. Seal, *J. Phys. Chem. B*, 2005, **109**, 3868.
30 J. Zhang, S. Y. Wei, J. Lin, J. J. Luo, S. J. Liu, H. S. Song, E. Elawad, X. Ding, J. M. Gao, S. R. Qi and C. C. Tang, *J. Phys. Chem. B*, 2006, **110**, 21680.
31 C. L. Lu, J. G. Lv, L. Xu, X. F. Guo, W. H. Hou, Y. Hu and H. Huang, *Nanotechnology*, 2009, **20**, 215604.
32 X. Y. Chen, H. S. Huh and S. W. Lee, *Nanotechnology*, 2007, **18**, 285608.
33 W. Q. Cai, J. G. Yu, S. H. Gu and M. Jaroniec, *Cryst. Growth Des.*, 2010, **10**, 3977.
34 Y. J. Zhu and L. Zhang, *J. Phys. Chem. C*, 2008, **112**, 16764.
35 J. G. Yu, W. Q. Cai, B. Cheng, B. L. Su and M. Jaroniec, *J. Phys. Chem. C*, 2009, **113**, 14739.
36 J. G. Yu, W. Q. Cai and M. Jaroniec, *J. Mater. Chem.*, 2010, **20**, 4587.
37 J. Zhang, S. J. Liu, J. Lin, H. S. Song, J. J. Luo, E. M. Elssfah, E. Ammar, Y. Huang, X. X. Ding, J. M. Gao, S. R. Qi and C. C. Tang, *J. Phys. Chem. B*, 2006, **110**, 14249.
38 Y. Zhu, H. W. Hou, G. L. Tang and Q. Y. Hu, *Eur. J. Inorg. Chem.*, 2010, 872.
39 Y. L. Feng, W. C. Lu, L. M. Zhang, X. H. Bao, B. H. Yue, Y. Iv and X. F. Shang, *Cryst. Growth Des.*, 2008, **8**, 1426.
40 T. Kim, J. B. Lian, J. M. Ma, X. C. Duan and W. J. Zheng, *Cryst. Growth Des.*, 2010, **10**, 2928.
41 H. Deng, X. L. Li, Q. Peng, X. Wang, J. P. Chen and Y. D. Li, *Angew. Chem., Int. Ed.*, 2005, **44**, 2782.
42 W. Stöber, A. Fink and E. Bohn, *J. Colloid Interface Sci.*, 1968, **26**, 62.
43 E.D., K. S. W. Sing., R. A. W. Haul, L. Moscou, R. A. Pierotti, J. Rouquerol and T. Siemieniewska, *Pure Appl. Chem.*, 1985, **57**, 603.
44 N. N. Nassar, *J. Hazard. Mater.*, 2010, **184**, 538.
45 J. H. Wang, S. R. Zheng, Y. Shao, J. L. Liu, Z. Y. Xu and D. Q. Zhu, *J. Colloid Interface Sci.*, 2010, **349**, 293.
46 M. A. Ferrogarcia, J. Riverautrilla, I. Bautistatoledo and M. D. Mingorance, *Carbon*, 1990, **28**, 545.
47 A. J. Vucina-Vujovic, I. A. Jankovic, S. K. Milonjic and J. M. Nedeljkovic, *Colloids Surf., A*, 2003, **223**, 295.
48 K. G. Karthikeyan and H. A. Elliott, *J. Colloid Interface Sci.*, 1999, **220**, 88.
49 http://daling5202.blog.163.com/blog/static/1726915762010102911146933/.

This journal is © The Royal Society of Chemistry 2011

J. Mater. Chem., 2011, **21**, 16550–16557 | 16557